JOURNAL OF PROPULSION AND POWER
Vol. 27, No. 4, July–August 2011

Ion Thruster Performance Impacts due to Cathode Wear

Dan M. Goebel,* James E. Polk,† and Ioannis G. Mikellides‡
Jet Propulsion Laboratory, California Institute of Technology, Pasadena, California 91109

DOI: 10.2514/1.B34058

It has been observed in ion thruster wear tests that the discharge loss increases with time and that the thruster performance correspondingly degrades. This behavior is usually attributed to an enlargement of the accelerator grid apertures during the tests due to ion erosion, which increases the grid transparency and thereby reduces the neutral gas pressure inside the thruster and decreases the ionization efficiency of the plasma generator. An analysis of thruster life test data using a discharge plasma model shows that this mechanism is insufficient to explain the observed results. Tests at Jet Propulsion Laboratory in an ion thruster simulator used in a 16,000-h discharge cathode wear test show similar increases in discharge loss with time, in spite of the fact that there are no ion accelerator or grid apertures eroding and that the average pressure in the discharge chamber is essentially constant. Experiments show that increases in keeper orifice diameter cause increases in discharge loss, and this trend is reproduced by two-dimensional numerical simulations that show a reduced ion generation rate in the near-keeper plume region as the electrode eroded. This cathode-electrode erosion mechanism is likely responsible for roughly half of the total discharge loss increases observed in ion thruster life tests.

Nomenclature

A_k	=	keeper electrode collection area
A_1	=	gas loss area of thruster simulator
A_2	=	effective gas loss area of an ion thruster
I_b	=	beam current
I_d	=	discharge current
I_k	=	keeper current
I_p	=	plate current
k	=	Boltzman's constant
m	=	electron mass
n_e	=	electron plasma density
n_o	=	neutral gas density
Q_c	=	cathode neutral gas flow input
Q_{in}	=	total neutral gas flow input
Q_m	=	discharge chamber neutral gas flow
Q_{out}	=	neutral gas flow escaping thruster
T	=	grid transparency
T_e	=	electron temperature
V_d	=	discharge voltage
V_k	=	keeper voltage
v	=	average neutral velocity
η_d	=	discharge loss
η_m	=	mass utilization efficiency of an ion thruster
η_{ms}	=	mass utilization efficiency of the thruster simulator
ϕ_p	=	plasma potential

I. Introduction

INCREASES in the ion thruster discharge loss in the first several thousand hours of life have been observed in several thruster life tests [1–3]. The performance of the thruster is degraded by this increased loss, which usually ranges from 10 to 20% of the initial discharge loss level. Changes in the discharge loss early in life are normally attributed to rapid accelerator grid erosion, due to the grid self-alignment effects of direct impingement, and rapid chamfering of the sharp edge of the etch-induced cusp in the grid webbing, due to charge exchange ion erosion. This grid erosion increases the transparency to neutral loss, which decreases the neutral gas density in the discharge chamber. The discharge loss increases because the ionization probability in the discharge chamber is proportional to the neutral density. For thrusters in which the discharge current is regulated, the reduction in the neutral density in the discharge chamber causes a proportional decrease in the number of ions generated and the beam current. Thrusters that regulate the beam current to produce a nearly constant thrust level during changes in the discharge efficiency increase the discharge current and indirectly and slightly the discharge voltage, to increase the ionization rate. The reduction in the neutral density and the increase in the discharge power raise the electron temperature, which produces sufficient ionization to produce the required beam current. Higher discharge losses are then primarily due to the enhanced neutral excitation losses and energy convection to the anode due to the higher electron temperature [4].

An examination of the data from the NASA Solar Electric Propulsion Technology Applications Readiness (NSTAR) thruster 8200-h life test demonstration test (LDT) [1] and the NSTAR 30,000-h extended life test (ELT) [2] shows that the discharge loss increased by approximately 15% in the first 4000 to 5000 h of the tests, but these changes do not match the time scales of the observed accelerator grid aperture diameter changes. An analytical model of the plasma discharge [4] in these thrusters shows that neutral gas density changes by themselves account for only about one-third of the total discharge loss increases observed. Other observed changes in the thruster operation in these life tests, such as changes in the screen grid transparency and discharge voltage, together with the neutral density changes, account for only about half the observed discharge loss increases.

Similar discharge loss increases were observed early in a 16,000-h wear test [5] of a xenon ion propulsion system (XIPS) thruster discharge cathode assembly, performed in an ion thruster simulator in which changes in grid transparency to neutrals and ions did not occur. In these tests, the grids were replaced by a flat molybdenum plate, biased to collect ion current and spaced sufficiently from the anode wall to produce the correct neutral gas loss rate and neutral pressure in the discharge chamber. The ion current to a flat carbon probe inserted on-axis through the molybdenum plate was employed to regulate the ion production rate using a "beam current control" loop identical to that used to regulate the beam current and thrust

Presented as Paper 2009-4920 at the AIAA Joint Propulsion Conference, Denver, CO, 3–6 August 2009; received 28 June 2010; revision received 6 December 2010; accepted for publication 22 December 2010.

*Senior Research Scientist. Fellow AIAA.
†Principal Engineer, Electric Propulsion Group. Associate Fellow AIAA.
‡Senior Engineer, Electric Propulsion Group. Member AIAA.

level in ion thrusters by varying the discharge current set point to regulate the current to the probe. The operation of this thruster simulator closely resembles the behavior observed in complete ion thruster life tests [1–3,6]. When in the beam current control mode, the discharge current increased slowly with time to maintain the collected probe current (the "beam current"), and the discharge voltage changed only slightly, as observed in normal ion thruster tests. The discharge was operated for 5600 h in a "high-power" (HP) mode, in which the discharge current increased from an initial 18 to about 21 A. The increase in the discharge current in the HP mode corresponded to about a 14% increase in discharge loss. Subsequently, the discharge current was reduced to 10.3 A (a midpower mode) for 5400 h and to 3.8 A [a low-power (LP) mode] for 5200 h, during which the discharge currents and discharge loss remained nearly constant. Although there were no grid apertures eroding, and the average pressure in the discharge chamber was essentially constant in these tests, the keeper electrode was observed to wear significantly in the HP mode, and the surface of the cathode orifice was slightly textured during operation.

To examine this further, measurements of the discharge loss were made in the thruster simulator with two different cathode keeper orifices. Because there is no beam generation in this system, the performance was analyzed using a modified version of the technique developed by Brophy [7] for simulating ion thruster performance without beam extraction. The discharge loss was observed to increase with the larger keeper orifice diameter in the HP mode, but the opposite effect occurred in the LP mode that was operated at about half the discharge current. Because most wear tests start in the highest-power state, in which the electrode erosion rates are the highest, keeper wear usually occurs at this time and contributes to the increased discharge loss observed.

These results clearly indicate that discharge loss increases in ion thrusters are due to many effects simultaneously occurring. The traditional interpretation of grid-wear-induced changes in the neutral pressure in the discharge chamber with time is credible, but it only accounts for about a third of the discharge loss increases observed. Changes in screen grid transparency can account for another fraction, and discharge voltage increases will account for an additional fraction if they are due to changes in the cathode insert that require higher operating temperatures. Changes in cathode keeper electrode shape will also increase the discharge loss at high cathode current densities. Later in life, when all these effects would normally contribute to a higher discharge loss, operation at lower thruster throttle points will cause the keeper electrode erosion effects to reduce the discharge loss. This mechanism tends to stabilize the discharge loss later in life in previous ion thruster life tests. Changes in the keeper material to reduce wear will reduce the discharge loss increases early in life, but they will also reduce the stabilization of the discharge loss later in life by this mechanism in actual thruster operation.

II. NSTAR Discharge Loss Trends

Wear tests of the NSTAR ion thruster [8] have shown an increase in the discharge loss with run time during the test [1,2]. For example, Fig. 1 shows the discharge loss vs time from the NSTAR LDT [1], which was run for 8200 h in the HP throttle level 15 (TH15) mode at 2.3 kW. The discharge loss was observed to increase by 10 eV/ion in the first few hundred hours from an initial value of about 172 eV/ion. The discharge loss then continued to increase fairly linearly for the next 4000 h, stabilizing at about 202 eV/ion. This represents an increase of 30 eV/ion over the first 4000 h, which is about a 15% increase that occurs early in the life of the thruster. Polk et al. attribute [1] the discharge performance degradation to wear of the accel grid orifice wall (so-called barrel erosion), which increased the neutral loss rate in the thruster.

Similar behavior of the discharge loss with time was observed in the 30,000-h ELT [2] of the NSTAR flight spare thruster from the Deep Space 1 mission. Figure 2 shows the discharge loss plotted as a function of time during the entire test [6], which included operation at several throttle levels. The discharge loss increased by about

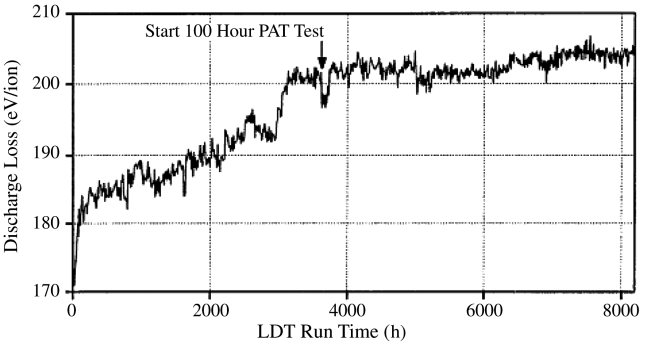

Fig. 1 LDT discharge loss vs run time in the TH15 HP throttle condition (from [1]).

10 eV/ion in the first few hundred hours, and then it increased at a nearly constant rate for several thousand hours to about 205 eV/ion. This is again approximately a 15% increase in the discharge loss early in the life of the thruster. The discharge loss in the HP TH15 mode then became essentially constant through the remainder of the test. Again, the increase in the discharge loss early in life was attributed to accel grid hole wear that increased the optical transparency of the grid and reduced the neutral gas density in the discharge chamber. However, observations of the accel grid hole diameter made during the test [6], which are plotted in Fig. 3, showed that the accel grid hole diameter increased rapidly in the first 1500 h of the test and then increased with a different slope with a nearly constant rate up to about 12,000 h. Beyond that time, the change in the ion optics due to the grid hole changes caused the charge exchange ions to hit primarily downstream of the accel grid centerline, causing chamfering of the hole but no increase to the minimum diameter of the hole.

Although both tests showed similar trends in discharge loss increase (≈15%) with time and attributed the behavior to lower neutral pressures in the discharge chamber from accel grid barrel erosion, the time scale of the discharge loss change is significantly shorter than the accel grid hole diameter changes. In fact, the accel grid hole diameter continued to increase due to erosion, whereas the discharge loss flattened and remained constant after 5000 h. It appears that other mechanisms need to be investigated to explain this discharge performance behavior.

Discharge loss is determined by the interaction of many different parameters in the thruster [4,5]. However, the strongest dependencies for a fixed discharge chamber geometry are in the screen grid transparency and the discharge voltage. This is because the screen grid transparency directly affects the number of ions that must be produced, and, because the discharge loss is typically an order of magnitude higher than the cost of producing a single ion, lower screen transparencies drive proportionally higher discharge losses. In addition, the discharge voltage strongly influences the ionization rate by changing the primary and secondary electron energies. An examination of the data from the LDT [1] shows that the screen grid

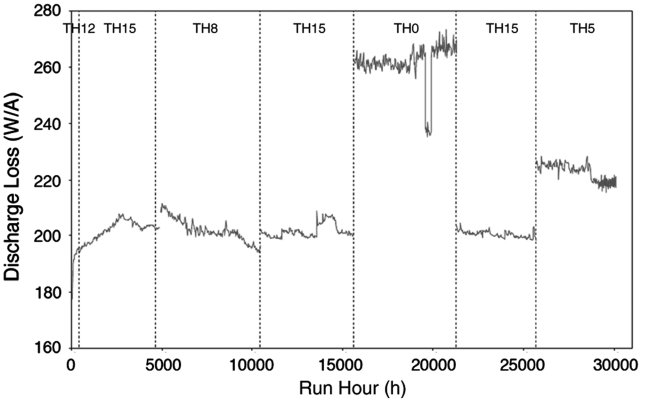

Fig. 2 Discharge loss vs run time in the ELT life test (from [6]).

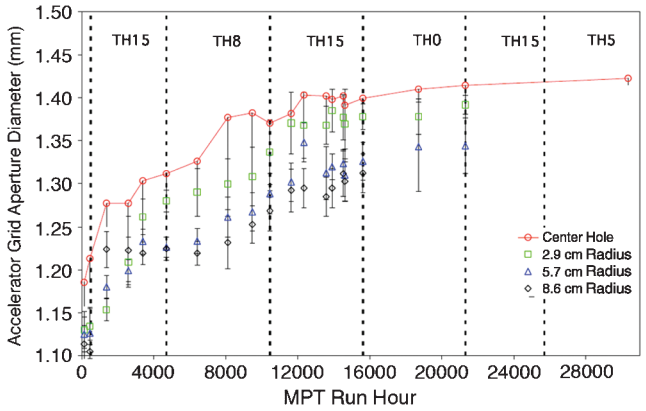

Fig. 3 ELT accel grid diameter vs run time (from [6]).

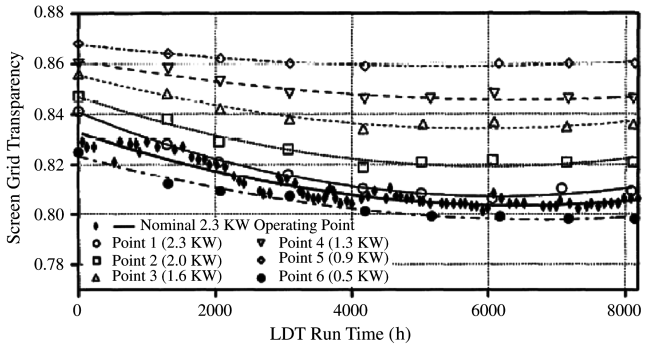

Fig. 4 LDT screen grid transparency vs run time (from [1]).

transparency decreased by about 2% over the first 4000 h of the test and then flattened with time, as seen in Fig. 4. Nearly identical behavior was observed in the ELT [2]. This grid transparency reduction will tend to increase the discharge loss on the same time scales, as observed in the life tests. In addition, the discharge voltage increased over the first 4000 h of the test, which would decrease the discharge loss if it resulted in more power delivered into the discharge chamber. Because the accel grid transparency increase does reduce the neutral density in the discharge chamber and increase the discharge loss, these effects are competing in determining the actual change in engine performance.

III. Discharge Loss Modeling Results

A zero-dimensional, self-consistent analytical discharge model has been previously developed [9] that can provide insights into the impact of changes in neutral pressure, screen transparency, discharge voltage, and other thruster parameters on the discharge loss. Figure 5 shows the discharge loss points, measured near the beginning of life (BOL) on an NSTAR thruster copy at Jet Propulsion Laboratory (JPL), and two predictions from the zero-dimensional analytical model for the BOL 83% screen grid transparency and the 81% screen grid transparency (dashed line) measured after 4000 h in the LDT and ELT. The 2% reduction in screen grid transparency by itself causes a 7.5 eV/ion increase in the discharge loss (<4%) at the nominal 90% mass utilization efficiency, at which the NSTAR engine runs in the TH15 mode. This is clearly insufficient by itself to explain the increases in discharge loss observed in the life tests.

The erosion of the accel grid for 4000 h in the ELT increased the barrel minimum diameter on-axis by about 13%. This causes the optical transparency of the accel grid near the centerline to increase from the BOL value of 24 to about 32%. However, the ELT data show that the accel grid aperture erosion decreases moving toward the grid edge, which is likely due to the large (>10:1) peak-to-edge density profile in the NSTAR thruster. Using the measured grid erosion at several radial points and weighting the aperture diameter change with the radius gives an average accel grid transparency at 4000 h of about 28%. This increase in the grid open area directly affects the neutral gas pressure in the discharge chamber. Because the zero-dimensional model [9] includes analytical solutions for the gas flows and pressures, it was found that this increase in accel grid transparency reduced the xenon neutral density in the discharge chamber by about 15%. The input gas injected directly into the discharge chamber is regulated by the feed system, and the beam current is regulated by the electrical supplies, and so the plasma system responds to changes in neutral density by increasing the discharge current to produce the same number of ions going into the beam. The zero-dimensional model predicts that the discharge loss increases about 9 eV/ion, due solely to the accel grid holes enlarging. Likewise, an increase in the discharge voltage by itself from 24.5 to 25 V reduces the discharge loss by about 3 eV/ion.

Including all three observed effects over the first 4000 h of the life tests, the screen grid transparency decrease, the accel grid transparency increase, and the discharge voltage increase raise the discharge loss by about 14 eV/ion at the nominal 90% mass utilization efficiency operating point. This is shown in Fig. 6, in which the discharge loss curves are plotted for the BOL and modified conditions listed previously. The discharge model shows that the observed modifications in the thruster geometry and operating characteristics are insufficient to explain the discharge loss change over the first 4000 h of thruster life. These effects combined are likely responsible for only about half the observed discharge loss change. An additional degradation mechanism early in life is needed.

IV. Additional Discharge Loss Mechanisms

There are two cathode-related mechanisms that increase discharge loss. First, self-heated cathodes automatically adjust the internal

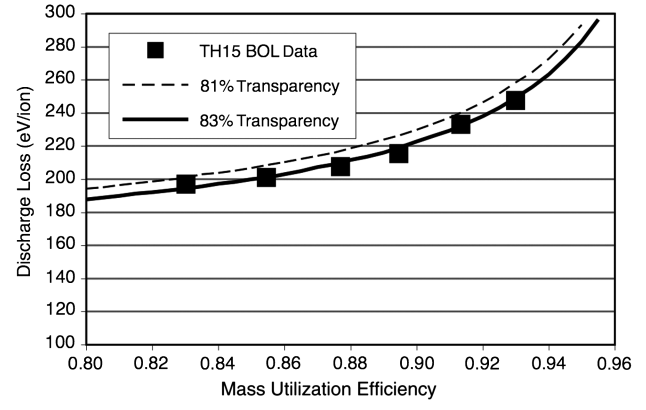

Fig. 5 NSTAR thruster discharge loss dependence on screen grid transparency.

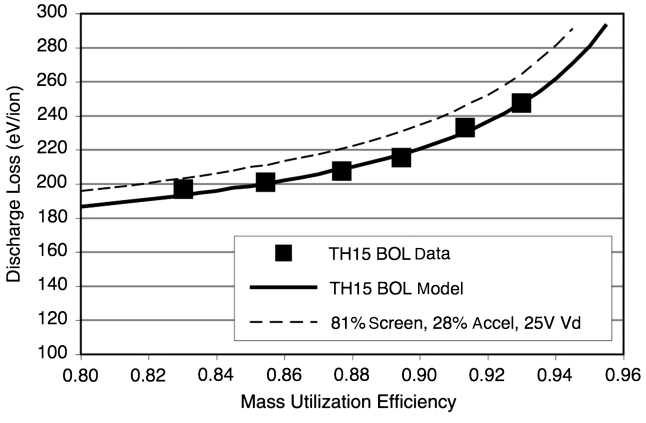

Fig. 6 NSTAR thruster discharge loss change with screen, accel, and discharge voltage changes observed in the life tests at 4000 h.

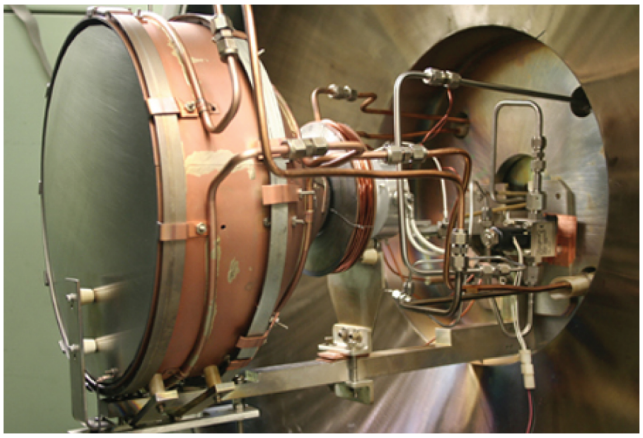

Fig. 7 Ion thruster simulator in the vacuum facility.

plasma potential in the insert region [4] to produce sufficient plasma heating to maintain the insert at the temperature required for adequate thermionic emission to supply the discharge current. The insert plasma potential is essentially a series voltage drop in the discharge power supply leg, which deposits heat in the cathode from the discharge supply as opposed to power delivered into the discharge chamber. Experiments [10] with fast-scanning miniature probes inserted directly into the insert region have measured these plasma potential changes as the discharge current and cathode gas flow rates are changed. In these experiments, it was found to be necessary to run the cathode for 100 to 200 h to get reproducible and stable plasma potentials, which represents conditioning of the cathode insert surface. The increase in internal plasma potential during this conditioning process was found to be equal to the increase in the discharge voltage observed during this time. In general, increases in discharge voltage early in the life of a hollow cathode, or after a cathode venting and restarting, are due to changes in the voltage drop in the cathode required to satisfy the self-heating conditions. This is a part of cathode conditioning in the presence of the plasma discharge.

The effect on the thruster discharge of cathode insert conditioning is to reduce the power delivered to the discharge chamber plasma only if the discharge current is regulated, which reduces the ionization rate and beam current. If the beam current is regulated in the thruster, then the discharge voltage or current will increase to make up the lost power required to produce the beam current. Assuming that the 0.5 V discharge voltage increase observed in the first 4000 h of the ELT was an increased voltage drop in the cathode, the zero-dimensional discharge model finds that the discharge loss would increase 4.2 eV/ion. Including this effect with the 2% screen transparency reduction, the 4% accel grid transparency increase and the final discharge voltage of 25 V cause a total increase in the discharge loss by 21.8 eV/ion or about 10%.

Another potential mechanism is cathode electrode erosion. The thruster life tests are typically run at the highest power early in the test, which tends to cause the most cathode electrode erosion. Changes to the cathode orifice or the keeper orifice can change the local neutral density, electron current density, plasma potential drop, and electron temperature. This can increase or decrease the discharge loss, depending on the detailed conditions in the cathode plume. Of primary interest is the impact of keeper electrode erosion, because keeper wear has been observed and documented in both the NSTAR [1,2] and XIPS [11] life tests. Significant chamfering of the downstream keeper electrode orifice edge was observed at the end of the LDT [2], and analysis [12] of the ELT life test data showed that the keeper erosion started immediately in the HP TH15 mode and produced chamfering of the downstream keeper edge, which increased with time until the upstream edge of the orifice was reached, at which point the diameter of the keeper orifice was observed visually to increase with time [2].

V. Laboratory Discharge Loss Experiments

Investigations of the effect of keeper electrode wear on thruster discharge loss were performed in an ion thruster simulation facility at JPL used in the 16,000-h discharge cathode life test [6]. A detailed description of this facility is given in the references on this test. The simulator is a laboratory copy of the 25-cm XIPS discharge chamber [13,14] configuration with a solid molybdenum plate at the normal screen grid location. The magnetic field at the cathode is produced in this setup by a solenoidal coil, used for other tests of the impact of cathode field strength on performance. A photograph of the test arrangement is shown in Fig. 7. The current to the biased plate at the discharge chamber exit is monitored to determine the total beam current that could be extracted by an ion optics system placed in this location with a given transparency. The current to a flat 1-cm-diam graphite disk probe, biased 20 V negative relative to cathode and mounted in the center of the plate facing the discharge region, is monitored and used by a feedback look with the discharge supply to simulate beam current regulation. The total current collected by the plate can also be used for feedback regulation but requires that the plate be biased negative with respect to the cathode, and sputtering at this bias causes a significant amount of molybdenum deposition on the anode wall, which can flake. The electrical circuit of this thruster simulator [6] with the feedback loop is shown in Fig. 8. The cathode gas flow is determined by the XIPS thruster throttle table previously developed [15], and the amount of gas injected into the discharge chamber is adjusted along with the gap between the discharge chamber wall and the end plate to produce the same neutral gas density as in the operating thruster. Figure 9 shows the discharge current and voltage during the first 5600 h of operation in the HP mode. After an initial checkout at 21 A of discharge current, the system was run for the first 1200 h with the discharge current regulated to 18 A. It was observed in this mode that the discharge

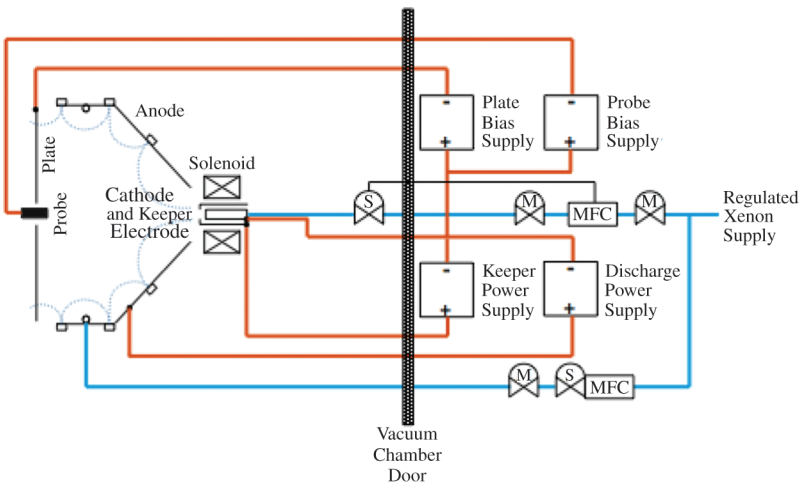

Fig. 8 Ion thruster discharge simulator electrical schematic.

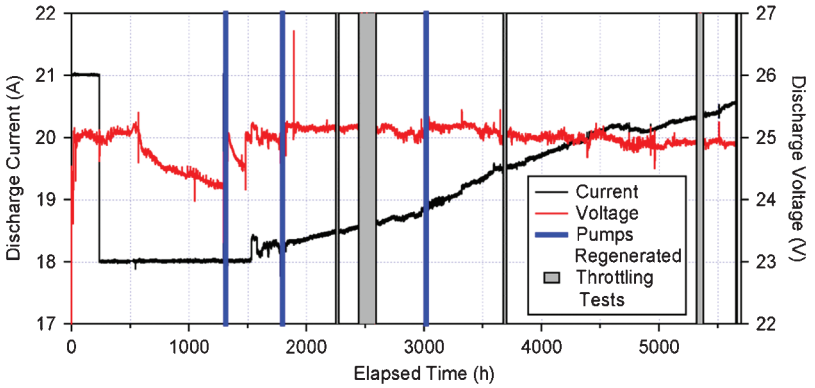

Fig. 9 Discharge current and voltage behavior in the ion thruster simulator in the HP mode (from [6]).

impedance decreased with time. However, the current to the front plate also decreased, indicating that although it was easier to produce the 18 A (lower discharge voltage), the thruster became less efficient in producing ions. At 1500 h, the regulation was switched to the beam control mode. From this point on, the discharge voltage remained essentially constant, and the discharge current increased with time for the remainder of the operation at this power level. This is identical to the behavior of ion thrusters with beam extraction in the beam current regulation mode, and it is indicative of an increase in discharge loss with time.

Analysis of the performance and discharge loss of a thruster without ion beam extraction was first developed by Brophy [7] in 1990. However, this analysis depended on knowledge of the ion collection by the cathode-potential biased accel grid and the subsequent neutral backflow fraction into the discharge chamber from the grids. In our experiments with the thruster simulator, the grids are replaced by a flat molybdenum plate, and all the ions incident on the plane in which the screen grid is normally located neutralize on the plate and return to the discharge chamber. Gaps between the edge of the plate and the discharge chamber wall and between the cathode structure and the discharge chamber wall were adjusted such that the nominal cathode flow rates and a small "main" flow injected into the discharge chamber produce approximately the same neutral gas pressure inside as in an operating thruster. Analysis of the discharge loss is then simplified, as will be shown next.

Discharge loss is defined as the total power into the discharge divided by the beam current:

$$\eta_d = \frac{I_d V_d + I_k V_k}{I_b} \tag{1}$$

in which I_d is the discharge current, V_d is the discharge voltage, and I_b is the beam current. To find the discharge loss in the simulator, the discharge current and voltage were measured and the bias voltage scanned on the front plate to find the saturated ion current. This ion current to the front plate was multiplied by factor for the transparency of a typical grid set to obtain an effective beam current. The keeper discharge power, which is typically about 10 W in these experiments, was measured and included in evaluating Eq. (1). A change in the assumed grid transparency simply displaces all the calculated discharge loss curves (discharge loss vs mass utilization efficiency) vertically.

The thruster simulator was configured to run at the same discharge voltage and current as the XIPS thruster [15] and to produce the same neutral density in the discharge chamber. In the thruster simulator, the neutral flow input (in particles per second) is equal to the neutral flow out though the open areas of the discharge chamber:

$$Q_{\text{in}}(\text{simulator}) = Q_{\text{out}} = \frac{1}{4} n_o \bar{v} A_1 \tag{2}$$

in which n_o is the average neutral density, v is the neutral gas velocity, and A_1 is the simulator discharge chamber open area. In an ion thruster, most of the neutral gas injected into the discharge chamber becomes beam ions, and only a small fraction is lost as neutrals. The neutral gas flow out of the thruster is then

$$Q_{\text{out}}(\text{thruster}) = Q_{\text{in}}(1 - \eta_m) = \frac{1}{4} n_o \bar{v} A_2 \tag{3}$$

in which η_m is the mass utilization efficiency and A_2 is the effective neutral loss area of the thruster. The total neutral flow into the thruster can be written as

$$Q_{\text{in}} = Q_c + Q_m = \frac{I_p T}{e} \frac{1}{\eta_m} \tag{4}$$

in which I_p is the total ion current to the plane of the screen grid, which is equivalent to the plate current in the thruster simulator, e is the charge, Q_c is the cathode flow rate, and Q_m is the main flow into the discharge chamber.

Equating the neutral densities in the thruster and simulator in Eqs. (2) and (3) and using Eq. (4) gives an expression for the mass utilization efficiency in the simulator as a function of the measured plate current:

$$\eta_{\text{ms}} = \frac{1}{\left(\dfrac{Q_{\text{in}} e}{I_p T} \dfrac{A_2}{A_1} + 1\right)} \tag{5}$$

In this equation, it is assumed that the neutral velocities are the same in the simulator and thruster, and the neutral flow, normally measured in standard cubic centimeters per minute (sccm), must be multiplied by a factor of 0.0722 to convert to equivalent amperes [4], if the plate current is in amperes. The equal neutral velocity assumption is justified, because the temperature of the large plate area in the simulator is about 205°C, which is nearly the same as the temperature of the operating thruster, and so the neutral temperatures should be similar.

The effective neutral loss areas in Eq. (5) can be readily calculated. The thruster simulator discharge chamber is inserted inside the vacuum system, and so any opening in the discharge chamber wall is a neutral loss area. The gap between the ion-collecting plate outside diameter and the discharge chamber inside diameter has an area of 76.5 cm^2. There is also a gap between the cathode keeper and the discharge wall of 20.3 cm^2, and so $A_1 = 76.5 + 20.3 = 96.8$ cm^2. The effective neutral loss area in a thruster is the total grid area times the optical transparency of the accel grid. For the 25-cm-diam XIPS thruster, the grid's neutral loss area is the hole-array area of 490.9 cm^2 times the BOL optical transparency of 24%, which is an effective area A_2 of 118 cm^2. The average neutral density in the thruster or the simulator at the HP condition, from Eq. (2), is

$$n_o = \frac{4(Q_c + Q_m)}{\bar{v} A_1} \tag{6}$$

in which the flow rates must be expressed in atoms per second, which is found by multiplying the flow in sccm by 4.47×10^{17}. The thermal velocity of xenon atoms at 205°C is 278 m/s. The average neutral

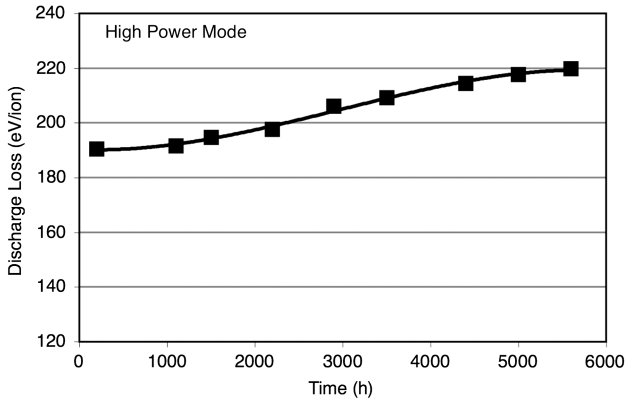

Fig. 10 Discharge loss in the thruster simulator in the HP mode as a function of time.

density in the discharge chamber from Eq. (6) in the HP mode is then 3.2×10^{18} m^{-3}. This is about the same average neutral gas density as found in the XIPS thruster in the HP mode, according to the zero-dimensional discharge model.

During the discharge cathode wear test, the discharge loss increased as a function of time in the HP mode. This is shown in Fig. 10, in which the discharge loss is calculated using Eqs. (1) and (5). The discharge loss increased by about 15 eV/ion over this period, consistent with the discharge current increase in Fig. 9 from 18 to 20.5 A. The neutral gas flow rates and pressure in the discharge chamber were regulated, and so the change cannot be attributed to grid erosion and neutral density changes.

During the cathode wear test, the keeper orifice diameter was observed to increase by over 13% during the first 5600 h of operation in the HP mode [6]. In this mode, the emitted discharge current started at 18 A and in the beam regulation mode increased to about 21 A over the 5600-h run time. The discharge loss curves, calculated using Eq. (5) for the beginning of the test with the nominal keeper orifice diameter and at the end of the HP mode phase at 5600 h with the keeper diameter enlarged by 13.8%, are shown in Fig. 11. In these tests, the discharge voltage was maintained at 25 V and the total current to the plate regulated to the value at the nominal XIPS discharge chamber mass utilization efficiency of about 85%. At this nominal point, the discharge loss was found to increase by over 10 eV/ion, or roughly 5% of the total discharge loss, with the enlarged keeper diameter. As seen in the figure, the change in discharge loss was found to also increase with mass utilization efficiency over the range that could be obtained with this setup. This is indicative of a reduction in ionization efficiency in the discharge chamber as the internal neutral density decreases, which is consistent with the expectation from the zero-dimensional discharge model results. Both cathode keeper diameter and internal neutral gas density are seen to impact the discharge loss.

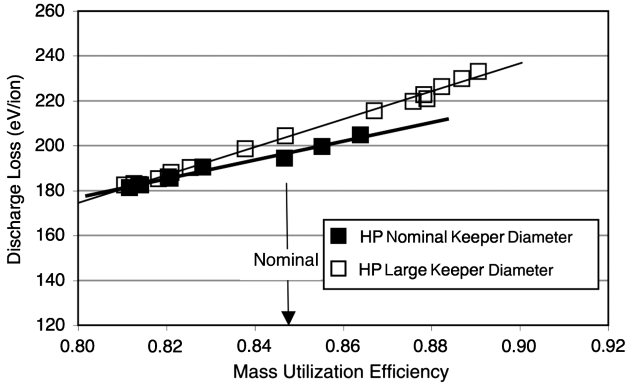

Fig. 11 Discharge loss for the HP mode in the thruster simulator for the nominal keeper orifice diameter and for the enlarged diameter found after 5600 h.

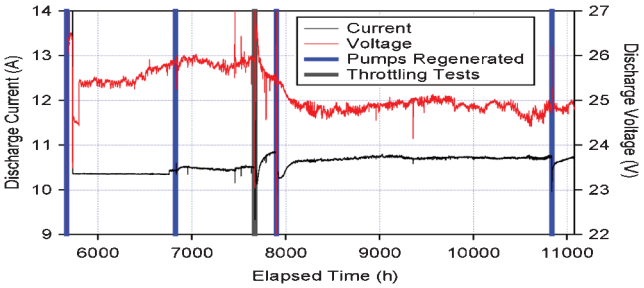

Fig. 12 Discharge current and voltage behavior in the ion thruster simulator in the medium-power 10.3 A mode for 5400 h of operation (from [6]).

The discharge cathode life test was also operated in a lower current, 10.3 A mode, for the next 5400 h of the test [6]. The discharge current and voltage behavior during this phase is shown in Fig. 12. The discharge was operated in the discharge current regulation mode for the first 2000 h. During this time, the discharge voltage and current were essentially stable, with small changes associated with the facility heating and cooling. After 2000 h, the system was switched to the beam current control mode. After a short period, required to stabilize the discharge after the regeneration of the pumps, the discharge current and voltage were both essentially constant for the remainder of this part of the test. Because negligible erosion of the keeper was observed during this period of operation [6], the discharge loss did not change significantly.

However, it is interesting to note that the direct effect of the enlarged keeper orifice produced in the HP before this phase was to reduce the overall discharge loss at the lower-power point. This is shown in Fig. 13, in which the discharge loss curves calculated using Eq. (5) from the thruster simulator data are plotted for the nominal keeper diameter and for the enlarged diameter measured at the start of this period of the tests. The discharge loss is decreased by about 10 eV/ion at the nominal operating condition of the thruster, which represents about a 5% improvement in the performance. This is indicative of better ionization efficiency of the system with a larger keeper orifice, which only occurs at lower-power levels.

VI. Dawn Flight Discharge Loss Data

Flight data from the Dawn mission using NSTAR ion thrusters are starting to become available [16,17] and are very important to this examination of various mechanisms for explaining the discharge loss changes during ion thruster operation. Figure 14 shows the discharge loss data vs thruster operating time from the three flight thrusters (FT1, FT2, and FT3) operating at their HP point (TH15 at 2.3 kW). The final performance data point from the ground testing is also shown, which was taken after approximately 50 h of burn-in and preflight testing. All three thrusters have discharge loss behavior that resembles the wear test results on this engine. The discharge loss

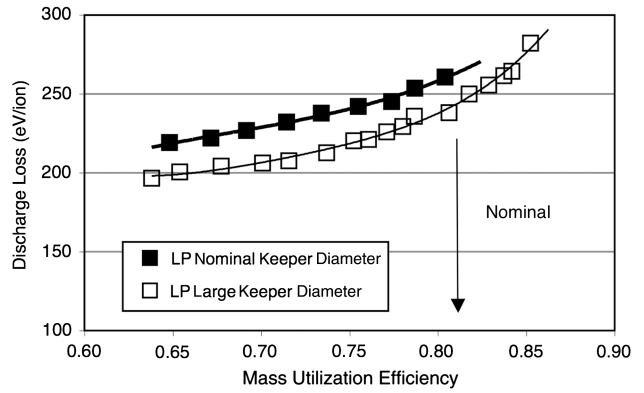

Fig. 13 Discharge loss curves in the thruster simulator for the lower-power 10.3 A case for two keeper orifice sizes.

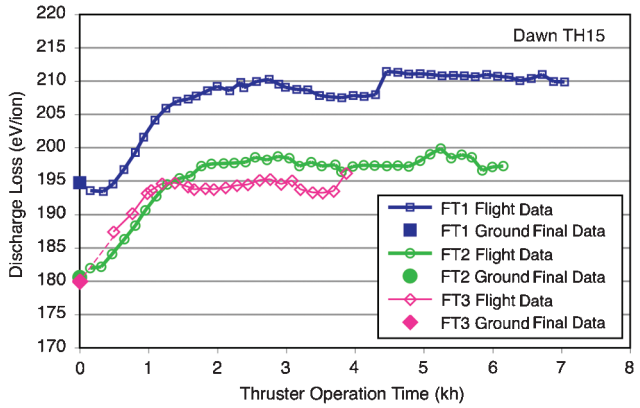

Fig. 14 Discharge loss as a function of thruster operating time at TH15 for the three Dawn thrusters in flight [17].

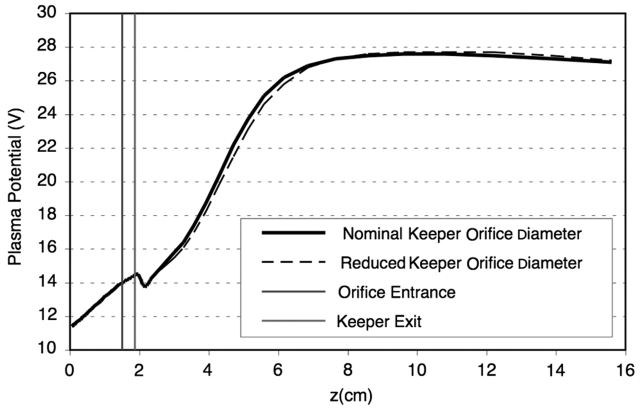

Fig. 15 Computed plasma potential along the axis of symmetry for the XIPS discharge hollow cathode at the nominal HP operating point. The plot compares results for two different diameters of the keeper orifice.

changes in the first 1000 to 3000 h of operation and then stabilizes. The increase in the discharge loss is about the same for all the thrusters (≈15 eV/ion) from the initial data point but is half that observed in both the ground wear tests (LDT and ELT). Although the FT1 thruster had a magnet orientation error that increased the magnitude of its discharge loss, the discharge loss behavior with time is similar to the other thrusters.

One possible explanation is that all these thrusters had the original NSTAR molybdenum keeper replaced by tantalum [18]. This material has a significantly lower xenon sputtering yield at low energy [19]. The NSTAR thrusters in Dawn are therefore expected to have much less keeper orifice wear than that observed in the original life tests with molybdenum keepers. A reduction in the keeper orifice wear would remove one of the discharge loss change mechanisms described previously and reduce the amount of change expected early in life. From the preceding analysis, any reduction in keeper wear in the HP mode would be expected to reduce the discharge loss by nearly a factor of two. Although this is not conclusive, it is consistent with the Dawn data associated with the use of the lower erosion-rate keeper material.

VII. Discussion

To better understand the trends observed in the cathode tests, we initiated a series of numerical simulations by extending the previous results [20] obtained for the XIPS discharge cathode at the nominal HP operating point. The simulations have been performed with the orificed cathode computer code OrCa2D, a two-dimensional axisymmetric model that simulates the partially ionized gas generated by these devices, both inside the cathode channel (in the insert region) and outside the channel, around the cathode orifice plate and the keeper region. The ion and electron current in the discharge are collected at a ring anode located at the downstream end of the physical domain. The simulation uses finite volume differencing to solve numerically the conservation equations for electrons, singly charged xenon ions, and xenon atoms, using a strongly implicit, time-split approach. OrCa2D has been applied in the past to simulate a variety of discharge [12,20] and neutralizer [21,22] hollow cathode geometries and operating conditions.

The results from the discharge loss tests described previously combine several effects, such as varying cathode and main flows at two different power levels and two different diameters of the keeper orifice. To isolate the impact of each effect on thruster performance, such as discharge loss, numerical simulations were performed at the high-power and medium-power operating points with no main flow and with fixed discharge current. Specifically, three keeper geometries were simulated: 1) nominal geometry; 2) a 28.6%-larger diameter, corresponding to the minimum diameter measured after 5600 h of operation in HP mode; and 3) a 50.8%-larger diameter, corresponding to a total keeper area exposed to the plasma, which approximately equaled the area at the end of the 5600 h. Although there is no significant change in the discharge voltage and plasma potential in the plume as the keeper orifice diameter changes, as shown in Fig. 15, a noticeable increase (of ∼3 V) in the keeper voltage is found for the case of the larger keeper diameter. The plasma potential profile is largely unchanged, because, for a given discharge current, the rise of the plasma potential in the discharge chamber is set largely by the competing resistive drop and electron pressure gradient, both of which are marginally affected by a change in the keeper orifice diameter. By contrast, the keeper voltage is driven by the current collection characteristics at the keeper, and these are strongly dependent on the available collection area and the plasma environment around the electrode. Specifically, our previous simulations with cathodes (especially neutralizers) have shown that

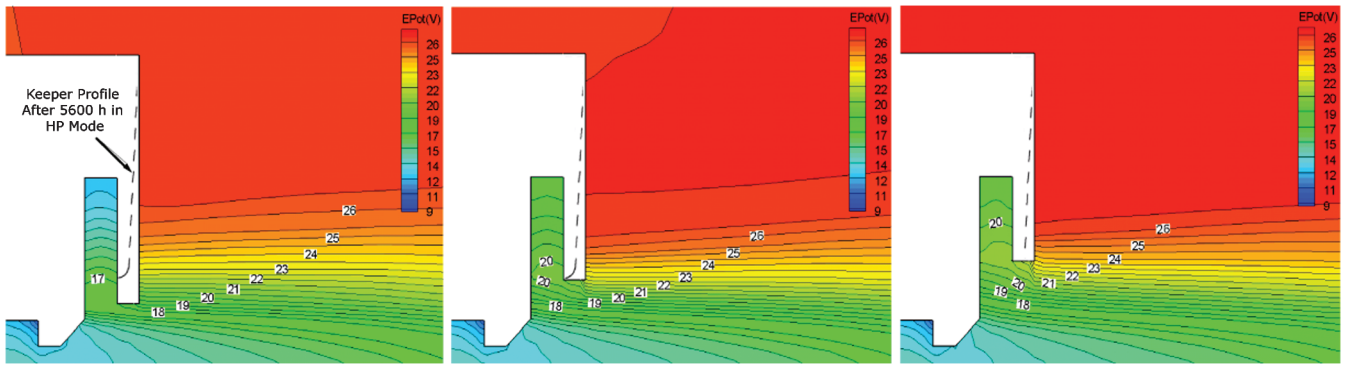

Fig. 16 Contour plots of computed plasma potential in the vicinity of the XIPS keeper electrode for the nominal keeper orifice diameter at the beginning of the test (left), a 28.6%-larger diameter corresponding to the minimum diameter measured after 5600 h of operation in HP mode (middle), and a 50.8%-larger diameter corresponding to a total exposed keeper area that approximately equals that of the test (right). The keeper shape measured after 5600 h is indicated by the dashed line.

Table 1 Change in thruster parameters for two simulation cases with enlarged keeper orifice diameters in HP mode: for a property S, unit changes are determined as $S_{\text{enlarged}} - S_{\text{nominal}}$, and percent changes are determined as $100 \times (S_{\text{enlarged}} - S_{\text{nominal}})/S_{\text{nominal}}$, in which the subscripts refer to the orifice diameter; changes in the local plasma conditions are computed near the middle of the inner surface of the keeper orifice

Parameter	+28.6% keeper diameter	+50.8% keeper diameter
Plasma potential, V	+2.5	+3.1
Electron temperature, eV	+1.0	+1.2
Electron number density $\times 10^{18}$, m^{-3}	−3.5	−4.1
Electron thermal current at orifice, %	−56.2	−69.1
Keeper voltage, V	+3.0	+3.6
Ion current at the outer boundaries, %	−5.9	−8.3
Discharge loss, %	+6.6	+9.3

most of the keeper current is collected primarily by the inner surface of the keeper orifice ring and that the largest contribution to this current is made by the electrons. The electron current to the keeper is proportional to

$$I_e \propto j_{\text{thermal}} \exp\left[\frac{-e(\phi - V_k)p}{kT_e}\right] A_k \tag{7}$$

in which the thermal electron current density is

$$j_{\text{thermal}} = \frac{1}{4} n_e \left(\frac{8kT_e}{\pi m}\right)^{1/2} \tag{8}$$

The difference between the plasma potential and the keeper potential ($\varphi_p - V_k$) is the sheath drop at the keeper electrode, and A_k is the keeper collecting area. For the larger keeper orifice the (∼40%) larger inner ring area available for electron collection requires less electron current density to the electrode to achieve a given current (assuming everything else is fixed), and this is partly attained in the thermal electron current contribution by the lower electron density in this region, because we compute approximately 75% decrease in the plasma density at the keeper orifice ring of the larger orifice.

However, the larger orifices are also exposed to regions of higher local plasma potential, as shown in Fig. 16, which tends to reduce even further the current density. This has a more significant effect, due to the sensitivity of the current density on the exponential. To compensate for this additional reduction in current density and retain a fixed value of the keeper current, the keeper voltage must increase. We compute an increase of about 3 V for this situation, which leads to a small increase in the discharge loss (less than 1%) because $I_k V_k$ is a smaller contribution to the total loss compared with $I_d V_d$.

With regard to discharge loss, integration of the ion current density over the areas of the ring anode and downstream exit boundary show a 5.9 and 8.3% reduction of the ion current in the cases of the 28.6%-larger and 50.8%-larger diameters, respectively. Including the changes in keeper voltage, the discharge loss for each of the two enlarged diameters is then increased by 6.6 and 9.3%. The second value is closer to the experimental value, because this keeper geometry has also approximately the same surface area as the eroded keeper. These and other relevant plasma values near the keeper orifice are tabulated in Table 1, to illustrate the changes that occur with the keeper orifice enlargement.

The numerical simulation results showed that the enlarging of the keeper reduced both the plasma density and neutral density in the near-plume region of the keeper, with a corresponding small change in the local electron temperature. The reduction of the neutral number density was found to be particularly significant, exceeding 60% in some locations near the keeper exit. Although the far-plume regions had essentially no change in the neutral gas density, because the values in these regions are driven by the unchanged total input flow and outer boundary conditions, the local neutral density reduction near the keeper led to the lower volumetric ion generation rate in the near-plume region. The resultant decrease in ion current in the far plume and the corresponding higher discharge loss are shown in Table 1. The fact that near-cathode plume ionization is a factor in the thruster performance is well known from observations that the use of strong axial magnetic fields at the cathode exit cause peaked plasma density profiles and improvements in discharge loss due to significant on-axis ionization. However, peaked plasma density profiles reduce grid life and perveance and increase the electron backstreaming threshold.

In the medium-power mode, the simulations showed that the keeper voltage increased 2.5 V relative to the HP mode, which was observed in the experiments, in order to collect the 1 A keeper current at the lower plasma density in the keeper region due to the lower discharge currents. The keeper voltage also increased due to a larger keeper diameter relative to the nominal at the start of the test, as was observed in the experiments. The discharge loss in the medium-power mode at a constant keeper diameter was found to increase by approximately 16% compared with the HP mode, due to lower neutral and plasma densities in the discharge chamber, and decrease as the keeper orifice eroded. All of these trends were observed in the experiments, and the simulations provide some insight into the mechanisms for these changes.

VIII. Conclusions

Several mechanisms for discharge loss changes observed early in the life of ion thrusters have been discussed. Changes in the internal neutral pressure due to grid erosion, changes in grid transparency, changes in discharge voltage, and changes in cathode electrode shapes due to erosion all contribute to the changes in discharge loss. Each of these mechanisms contribute some fraction of the total amount, depending on the magnitude of the change in each. Cathode keeper erosion is shown to increase the discharge loss in the high-discharge-current case and has the opposite trend effect at lower-discharge-current levels, in which the discharge loss decreases due to large keeper orifice diameters. Changes in the ionization efficiency of the hollow cathode discharge depend most strongly on the local neutral gas density in the near-cathode plume, which decreases as the keeper erodes and impacts the discharge loss.

Acknowledgment

The research described in this paper was carried out by the Jet Propulsion Laboratory, California Institute of Technology, under a contract with NASA.

References

[1] Polk, J. E., Anderson, J. R., Brophy, J. R., Rawlin, V. K., Patterson, M. J., Sovey, J., and Hamley, J., "An Overview of the Results from an 8200 Hour Wear Test of the NSTAR Ion Thruster," 35th Joint Propulsion Conference, AIAA Paper 1999-2446, Los Angeles, 20–24 June 1999.

[2] Sengupta, J. R., Anderson, J. R., Garner, C., Brophy, J. R., deGroh, K., Banks, B., and Thomas, T., "Deep Space 1 Flight Space Ion Thruster 30,000 Hour Life Test," *Journal of Propulsion and Power*, Vol. 25, No. 1, 2009, pp. 105–117. doi:10.2514/1.36549

[3] Herman, D., Soulas, G., and Patterson, M., "NEXT Long-Duration Test Plume and Wear Characteristics After 16,550 h of Operation and 337 kg of Xenon Processed," 44th Joint Propulsion Conference, AIAA

Paper 2008-4919, Hartford, CT, 21–23 July 2008.
[4] Goebel, D. M., and Katz, I., *Fundamentals of Electric Propulsion Ion and Hall Thrusters*, Wiley, New York, 2008.
[5] Polk, J. E., Goebel, D. M., and Tighe, W., "Ongoing Wear Test of a XIPS 25-cm Thruster Discharge Cathode," 44th Joint Propulsion Conference, AIAA Paper 2008-4913, Hartford, CT, 21–23 July 2008.
[6] Sengupta, A., Anderson, J., Brophy, J. R., Kulleck, J., Garner, C., deGroh, K., Karniotis, T., Banks, B., and Walters, P., "The 30,000 Hour Extended Life Test of the Deep Space Flight Spare Ion Thruster, Final Report," NASA TP-2004-213391, March 2005.
[7] Brophy, J. R., "Simulated Ion Thruster Operation Without Beam Extraction," 21st International Electric Propulsion Conference, AIAA Paper 1990-2655, Orlando, FL, 1990.
[8] Brophy, J., "NASA's Deep Space 1 Ion Engine," *Review of Scientific Instruments*, Vol. 73, No. 2, 2002, pp. 1071–1078. doi:10.1063/1.1432470
[9] Goebel, D. M., Wirz, R. E., and Katz, I., "Analytical Ion Thruster Discharge Performance Model," *Journal of Propulsion and Power*, Vol. 23, No. 5, 2007, pp. 1055–1067. doi:10.2514/1.26404
[10] Goebel, D. M., Jameson, K., Katz, I., and Mikellades, I., "Hollow Cathode Theory and Modeling: Plasma, 1. Characterization with Miniature Fast-Scanning Probes," *Journal of Applied Physics*, Vol. 98, No. 11, 2005, pp. 113302. doi:10.1063/1.2135417
[11] Tighe, W. G., Chien, K. R., Solis, Z., and Spears, R., "The 25 cm XIPS Life Test and Post Test Analysis," 31st International Electric Propulsion Conference, IEPC Paper 2009-161, Ann Arbor, MI, 20–24 Sept. 2009.
[12] Mikellides, I. G., Katz, I., Goebel, D. M., Jameson, K. K., and Polk, J. E., "Wear Mechanisms in Electron Sources for Ion Propulsion, 2: Discharge Hollow Cathode," *Journal of Propulsion and Power*, Vol. 24, No. 4, July–Aug. 2008, pp. 866–879. doi:10.2514/1.33462
[13] Chien, K. R., Tighe, W. G., DePano, M., Bond, T., and Spears, R., "L-3 Communications ETI Electric Propulsion Overview," 29th International Electric Propulsion Conference, IEPC Paper 2005-315, Princeton, NJ, 31 Oct.–4 Nov. 2005.
[14] Beattie, J. R., "Ion Propulsion Keeps Satellites on Track," *Industrial Physicist*, Vol. 4, No. 2, June 1998, pp. 24–26.
[15] Tighe, W. G., Chien, K. R., Solis, E., Robello, P., Goebel, D. M., and Snyder, J. S., "Performance Evaluation of the XIPS-25 cm Thruster for Application to NASA Missions," 42nd Joint Propulsion Conference, AIAA Paper 2006-4999, Sacramento, CA, 10–13 July 2006.
[16] Brophy, J. R., Garner, C., and Mikes, S., "Dawn Ion Propulsion System: Initial Checkout After Launch," 44th Joint Propulsion Conference, AIAA Paper 2008-4917, Hartford, CT, 20–23 July 2008.
[17] Garner, C., Rayman, M., and Brophy, J. R., "In-Flight Operation of the Dawn Ion Propulsion System Through Start of the Vesta Cruise Phase," 45th Joint Propulsion Conference, AIAA Paper 2009-5091, Denver, CO, 2–5 Aug. 2009.
[18] Brophy, J. R., Ganapathi, G., Garner, C., Gates, J., Lo, J., Marcucci, M., and Nakazono, B., "Status of the Dawn Ion Propulsion System," 40th Joint Propulsion Conference, AIAA Paper 2004-3433, Fort Lauderdale, FL, 11–14 July 2004.
[19] Doerner, R., White, D., and Goebel, D. M., "Sputtering Yield Measurements During Low Energy Xenon Plasma Bombardment," *Journal of Applied Physics*, Vol. 93, No. 9, 2003, pp. 5816–5823. doi:10.1063/1.1566474
[20] Mikellides, I. G., Katz, I., Goebel, D. M., and Polk, J. E., "Assessments of Hollow Cathode Wear in the Xenon Ion Propulsion System (XIPS) by Numerical Analyses and Short-Duration Tests," 44th Joint Propulsion Conference, AIAA Paper 2008-5208, Hartford, CT, 20–23 July 2008.
[21] Mikellides, I. G., and Katz, I., "Wear Mechanisms in Electron Sources for Ion Propulsion, 1: Neutralizer Hollow Cathode," *Journal of Propulsion and Power*, Vol. 24, No. 4, 2008, pp. 855–865. doi:10.2514/1.33461
[22] Mikellides, I. G., Goebel, D. M., Snyder, J. S., Katz, I., and Herman, D. A., "Neutralizer Hollow Cathode Simulations and Validation with Experiments," 45th Joint Propulsion Conference, AIAA Paper 2009-5196, Denver, CO, 2–5 Aug. 2009.

L. King
Associate Editor